Seismic hazard assessment in the Northern Andes (PILOTO Project)

Cristina Dimaté ([1]), **Lawrence Drake** ([2]), **Hugo Yepez** ([3]), **Leo Ocola** ([4]), **Herbert Rendon** ([5]), **Gottfried Grünthal** ([6]) **and Domenico Giardini** ([7]) ([8])

([1]) *Instituto de Investigaciones en Geociencias, Minería y Química (INGEOMINAS), Santsfé de Bogotá, Colombia*

([2]) *Observatorio de San Calixto, Bolivia*

([3]) *Escuela Politécnica de Quito (EPN), Quito, Ecuador*

([4]) *Instituto Geofísico del Perú (IGP), Perú*

([5]) *Fundación Venezolana de Investigaciones Sismológica (FUNVISIS), Caracas, Venezuela*

([6]) *GeoforschungsZentrum (GFZ), Potsdam, Germany*

([7]) *Institute of Geophysics, ETH, Zurich, Switzerland*

([8]) *Istituto Nazionale di Geofisica, Roma, Italy*

Abstract

Five Andean countries (Bolivia, Peru, Ecuador, Colombia, Venezuela) and four European countries (Italy, Spain, Holland, Germany) cooperated in the PILOTO program («Test area for earthquake monitoring and seismic hazard assessment»), launched under GSHAP and sponsored by the European Union (Ct.94-0103) to produce a unified SHA for the Andean region. Activities included the integration of national earthquake catalogues and source zonings in common regional databases and joint technical workshops for the assessment of the regional hazard, expressed in terms of expected peak ground acceleration with 10% exceedance probability in 50 years.

Key words *seismic hazard assessment – earthquakes – Andes – Sud-America – UN/IDNDR*

1. Introduction

The results presented in this summary were achieved during the execution of the Project EU-DG12 Ct. CI1* 94-0103: Pilot Project for Regional Earthquake Monitoring and Seismic Hazard Assessment (Andean and Mediterranean region), referred to as PILOTO. This project, proposed under the initiative of the Centro Regional de Sismología para América Latina (CERESIS) and supported by the European Community, was implemented over 3 years (1995-1997) and joined research organizations of 4 countries of the European-Mediterranean area (EUME) and 5 countries from the Andean Pact (JUNAC). The main goals of the project related to hazard assessment were to complete the compilation of the instrumental and historical earthquake catalogue for the JUNAC area, and to produce a regional seismic hazard assessment map in the JUNAC region adopting a common approach based on: i) joint work in multidisciplinary research and data; ii) the analysis of seismogenic structures without political boundaries, and iii) training a group of young scientists of the JUNAC countries in hazard assessment matters.

In this part of the project research was conducted for the following institutions: from the JUNAC countries Observatorio de San Calixto, Bolivia; Instituto de Investigaciones en Geo-

Mailing address: Dr. Cristina Dimaté, Instituto de Investigaciones en Geociencias, Minería y Química (INGEOMINAS), Santsfé de Bogotá, Colombia; e-mail: cdimate@esmeralda. ingeomin.gov.co

ciencias, Minería y Química (INGEOMINAS), Colombia; Escuela Politécnica de Quito (EPN), Ecuador; Instituto Geofísico del Peru (IGP), and Fundación Venezolana de Investigaciones Sismológica (FUNVISIS),Venezuela; from the EUME countries: GeoforschungsZentrum (GFZ), Germany; Institute of Geophysics, ETH, Switzerland; and Istituto Nazionale di Geofisica (ING), Italy.

The scope of the research and the strategy followed in order to achieve these tasks were defined among the PILOTO participants. It was agreed that the development of the seismic hazard map would be essentially an integration exercise aimed on building a common set of concepts, in defining jointly a seismic source zoning without political boundaries and in integrating past and ongoing national and regional initiatives. In no way this map would constitute an official seismic hazard map for the region, given that the official institution for seismic affairs in the region is CERESIS, the Regional Seismic Center for South America. Detailed description of the procedures and results achieved can be consulted in PILOTO Project (1997).

2. Tectonic setting of the Northern Andes

The North Western region of South America is characterized by two contrasting provinces from the geologic and geographic point of view: a relatively stable, low topography, region known as the South American platform, involving Central and Southern Venezuela, and Eastern Colombia, Ecuador, Peru and Bolivia; and a second region to the west, active and deformed, associated to the mountain chain of the Andes. The Andes extends as a single chain along the continental margin from Central Chile to Southern Bolivia where the Altiplano is developed up to Central Peru. From there north to Ecuador the Andes becomes again a single chain and in Colombia it splits in three chains, the easternmost continuing into Venezuela.

Tectonics of the region has been interpreted in terms of the convergence of the Caribbean, Nazca and South American plates. Interaction of these plates results in the deformation of the continental margin forming the belt of folded mountains that now constitute the ranges of the Andes. Relative motion between the Caribbean and South American plates at a rate of 14 mm/yr in direction ESE (Freymuller *et al.*, 1993) is absorbed mainly along an extended transform system conformed by the Boconó, Morón and El Pilar Faults in Venezuela and the Caribbean Deformed Belt in the coastal margin in Colombia.

Subduction of the oceanic Nazca plate under the South America plate in the Northern Andes takes place along the Colombia-Ecuador-Peru trench (Suárez *et al.*, 1993). These two plates converge in a N80°E direction at a rate of 78 mm/yr (de Mets *et al.*, 1990) giving rise to numerous great earthquakes along the margin. The subducted plate geometry inferred from the intermediate and deep seismicity indicates variations along strike associated to segmentation and buckling of subduction (Pennington, 1981; Jordan *et al.*, 1983; Norabuena *et al.*, 1994). The changes in geometry of subduction correlate to the presence and absence of the volcanic arc. Zones of subhorizontal subduction exists with the absence of volcanism, while normal angle subducting plate geometry is present with active volcanic arc.

Besides activity associated to plate boundaries, convergent tectonics originates active internal deformation in the Andean block evidenced by neotectonic activity and seismicity concentrations along the interandean valleys and coastal fault systems.

The relative motion between Caribbean, Nazca and South American plates is accommodated along the margins defining the regions where the major earthquakes occur. Nevertheless, the Andes represents a zone of wide spread deformation where the remaining convergence is adjusted. The Andes defines a zone of compression characterized by reverse faulting on the foothills (*e.g.*, Subandean, Colombian Llanos foothills) roughly perpendicular to the vectors of plate convergence, strike slip faults (*e.g.*, Oca fault, Pallatanga fault) and some normal faults on the high cordillera (*e.g.*, Cordillera Blanca fault). Seismicity clearly defines the deformation front of the previously mentioned zones.

3. Seismicity

3.1. *Earthquake catalogue for the Andean region*

The earthquake catalogue for the JUNAC countries (Bolivia, Colombia, Ecuador, Peru and Venezuela) used in PILOTO project was extracted from the Catalogue of Earthquakes for South America - SISRA project (CERESIS, 1985), hereon called CERESIS catalogue, which has been updated to December 1991 (CERESIS, 1996). The information on this was compiled by the representing institutions for CERESIS in each country. Since almost all the Andean institutions participating in PILOTO (excepting IGP) were the same ones that prepared the respective catalogues for CERESIS it was natural to use it in the project. In seismic hazard calculations the seismic data from Chile and Argentina, in the limits with Peru and Bolivia were included to have more realistic values of hazard.

A complete description of the hypocenter catalogue can be found in CERESIS (1985), and Tanner and Shepherd (1997). The following describing paragraphs were summarized from these two documents in order to describe the contents of the catalogue and the criteria taken into account while compiling it.

The catalogue spans from historical to instrumental events, including instrumental data from local agencies, observatories, stations and universities. It covers a time period beginning with the earliest known historical event for each country and ending December 1991, being the earliest event included from 1471. A total number of 18137 earthquakes are reported in the catalogue, all magnitudes included, for a time period of about 500 years. The completeness of the catalogue varies over time, being relatively incomplete for early historical events and much more complete for recent ones. The lower magnitude cut-off has been designated as 4.5 m_b. Smaller events have not been vigorously eliminated, particularly since many events have no reported or calculated magnitudes. The catalogue, however, is much less complete for events below magnitude 4.5 m_b. A two letter country code together with a five digit identifying number provide a unique reference for each event.

Quality factors for time, epicenter and depth has been associated for most of the events. Quality factors used by other sources for hypocenter data were converted to the factors defined for the catalogue. Space is provided for four magnitude values. The first is an m_b magnitude, followed by an M_S magnitude. The other two may be additional m_b or M_S magnitudes, other reported magnitudes, magnitudes derived from intensity data, or magnitudes converted from one scale to another. All intensities are listed in either the Modified Mercalli (MM) or the MSK scale.

In fig. 1 are plotted the events with magnitude equal or over 6.5 contained in the catalogue. The same is done in fig. 2 for events with magnitude lower than 6.5. For this catalogue a Gutenberg-Richter law gives a return period of 45 years approximately for events with magnitude over 8.0.

3.2. *Magnitude homogenization*

Given the importance of having a uniform and homogeneous parameter to compare size of earthquakes in the process of seismic hazard computations, the catalogue was examined in detail, magnitudes were homogenized to surface magnitude, M_S, and events without magnitude or with zero magnitude were removed.

To convert magnitudes different from M_S, to M_S, linear regressions between events with both magnitudes reported were calculated. The procedure was as follows:

i) Examination of type and quality of magnitude information for each country since they have been compiled independently. As result of this examination 20135 events were removed from the original catalogue, as shown in table I.

ii) Plotting histograms for the four types of magnitude reported in the CERESIS catalogue (m_b = body wave magnitude, M_S = surface wave magnitude, $M1$ and $M2$ other magnitudes) for each country.

iii) Calculation of regression equations and comparison with previous equations used in the CERESIS catalogue (figs. 3a,b).

iv) Conversion of magnitudes to M_S under the following criteria:

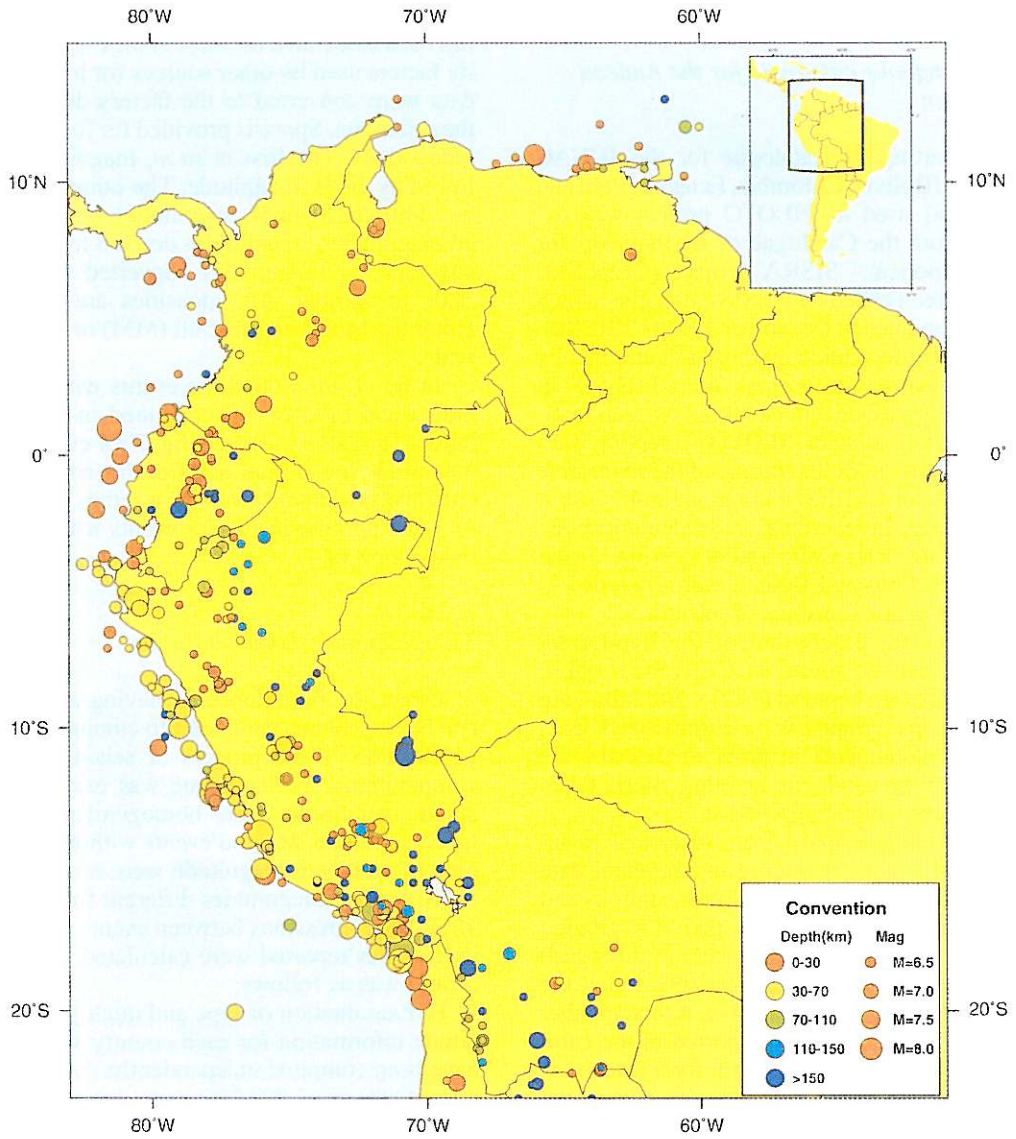

Fig. 1. Events with magnitude equal or over 6.5 in the North Andean region, extracted from CERESIS (1996).

1) For events with reported instrumental M_s magnitude that value is preserved.

2) For events with reported maximum epicentral intensity I_0, M_s is calculated using the standard Gutenberg and Richter equation (Gutenberg and Richter, 1956)

$$M_s = 1 + 2/3 \cdot I_0$$

except for Peru, where Huaco and Rodriguez's relations were used (CERESIS,1985).

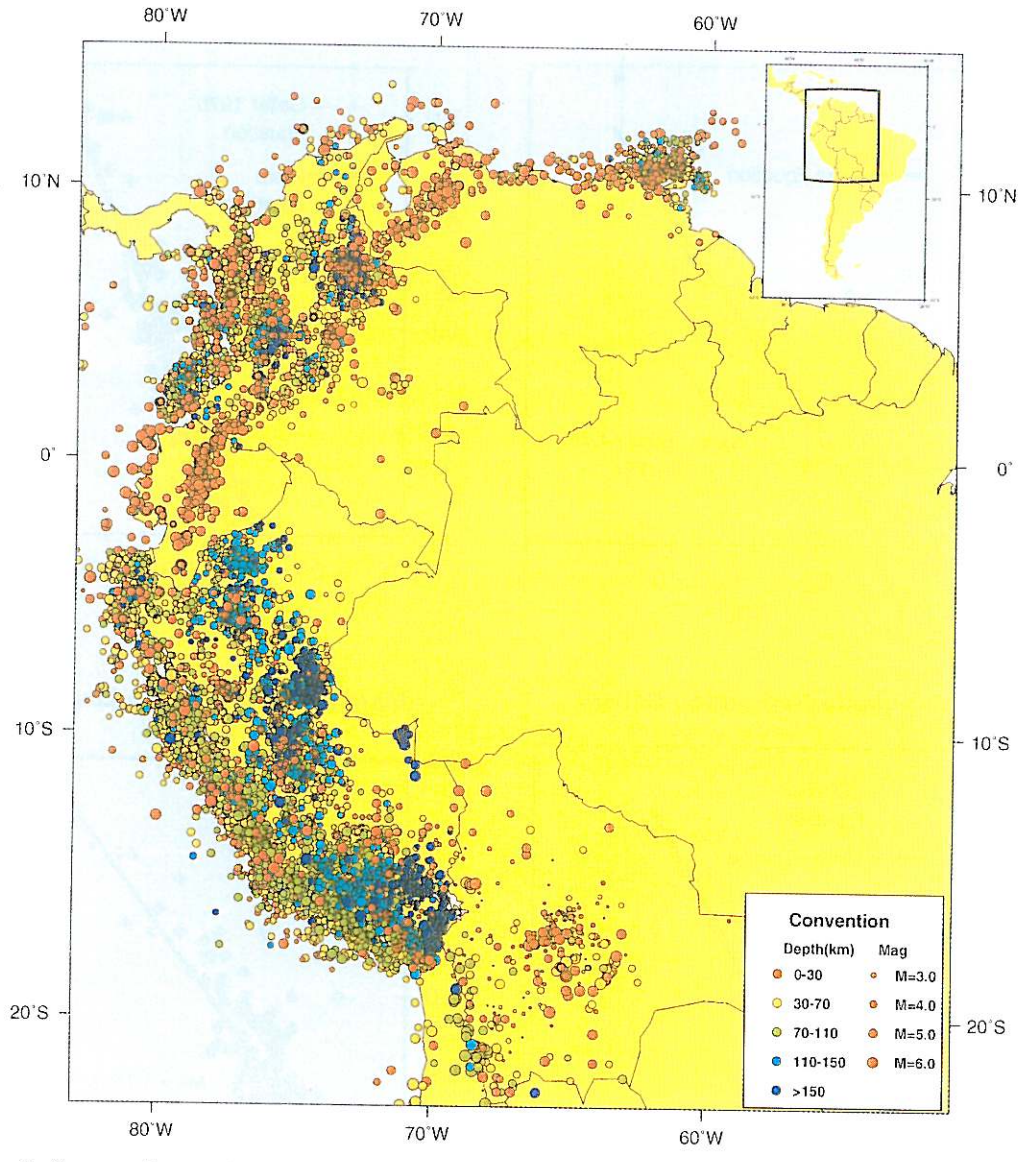

Fig. 2. Events with magnitude less than 6.5 in the North Andean region, extracted from CERESIS (1996).

Table I. Number of earthquakes for country in the regional catalogue.

Number of events	Bolivia	Colombia	Ecuador	Peru	Venezuela	Argentina	Chile
Removed	394	0	431	1013	1199	5255	11843
Final	831	3221	1758	6984	1880	3136	5288

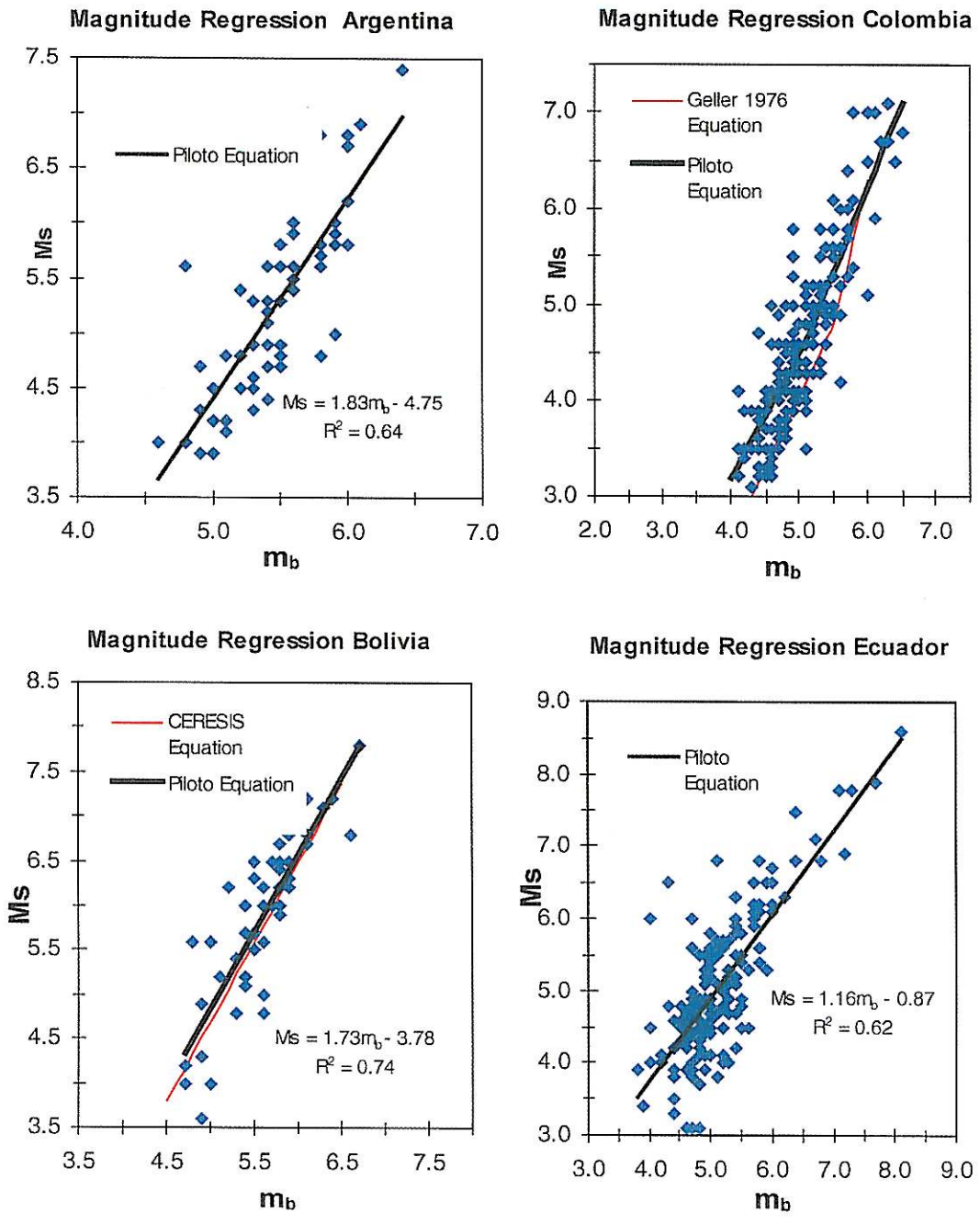

Fig. 3a. *M_s versus m_b* regression equations for Argentina, Colombia, Bolivia and Ecuador. Thin lines correspond to previous equations (CERESIS,1985), thick line to PILOTO equation.

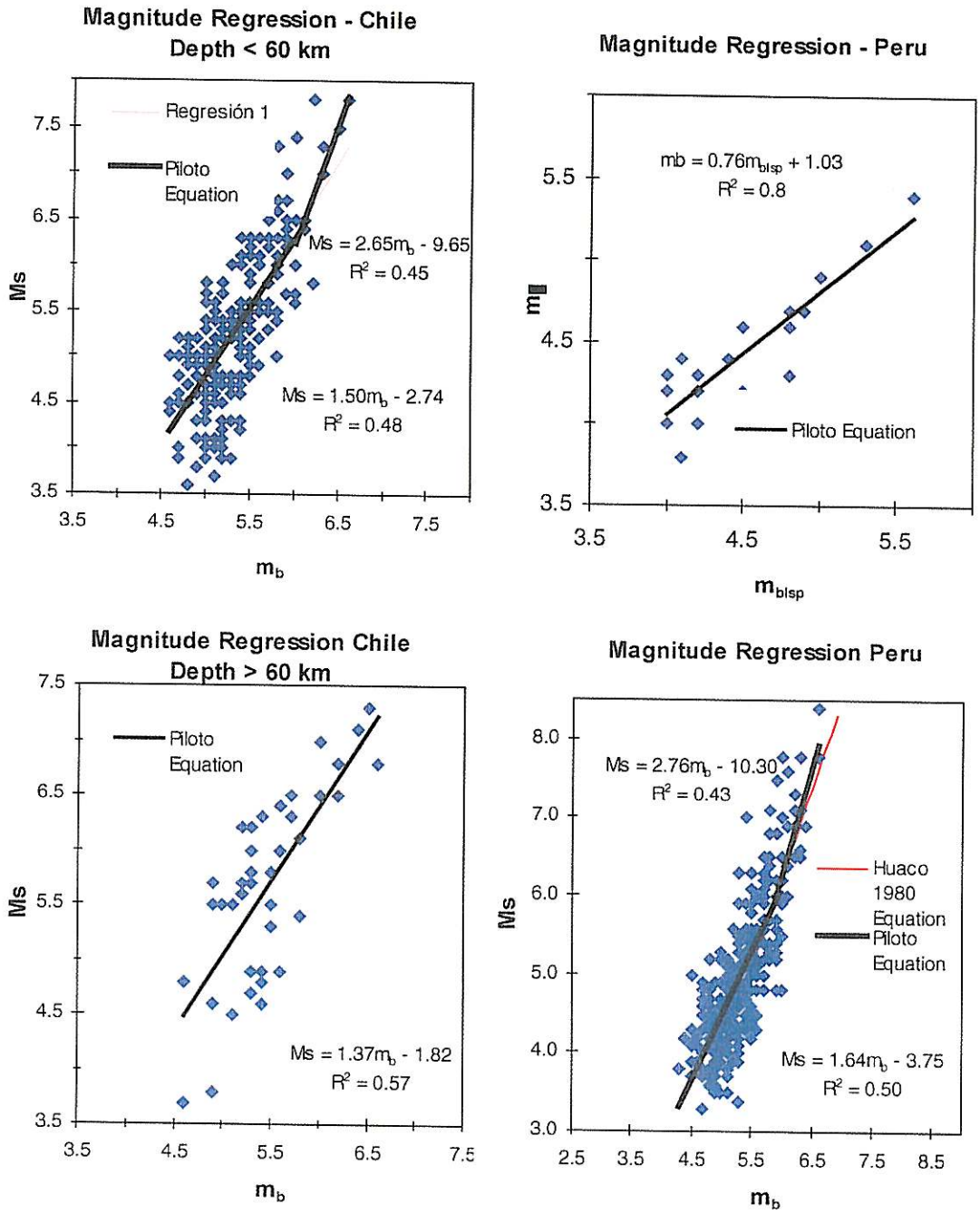

Fig. 3b. *M_s versus m_b* regression equations for Chile and Peru. Thin lines correspond to previous equations (CERESIS,1985), thick line to PILOTO equation.

3) For events with m_b magnitudes reported, M_S is calculated using the regression equations derived in (iii) for each country:

Argentina

$M_S = 1.116 \cdot m_b - 1.067$ $\quad m_b < 5.8$

Bolivia

$M_S = 1.786 \cdot m_b - 4.232$

Colombia

$M_S = 1.33 \cdot m_b - 2.13$ $\quad m_b < 5.2$
$M_S = 1.77 \cdot m_b - 4.42$ $\quad m_b \geq 5.2$

Chile

Depth < 60 km:
$M_S = 1.503 \cdot m_b - 2.737$ $\quad m_b < 6.0$
$M_S = 2.649 \cdot m_b - 9.653$ $\quad m_b \geq 6.0$

Depth ≥ 60 km:
$M_S = 1.369 \cdot m_b - 1.817$

Ecuador

$M_S = 1.157 \cdot m_b - 0.873$

Peru

$m_b = 0.757 \cdot m_{LSP} + 1.027$
$M_S = 1.644 \cdot m_b - 3.753$ $\quad m_b < 5.9$
$M_S = 2.763 \cdot m_b - 10.301$ $\quad m_b \geq 5.9$

Venezuela

$m_b = 0.742 \cdot m_{TRN} + 1.172$
$M_S = 1.116 \cdot m_b - 1.067$ $\quad m_b < 5.8$
$M_S = 2.714 \cdot m_b - 10.369$ $\quad m_b \geq 5.8$

For the Chilean catalogue best adjustment was obtained grouping the events in two ranges of depth: 0 to 60 km and greater than 60 km.

3.3. *Removal of dependent events*

To fulfill the requirements of a Poisson distribution, assumed as representative of the earthquake time occurrence distribution, removal of dependent events was performed. Since most of the dependent events are aftershocks, an algorithm was developed to remove them based on Maeda's relation (1996). These relations establish spatial and temporal criteria to eliminate aftershocks from the original data as follows:

- as for distance: $L \leq 10^{(0.5\,Mm - 1.8)}$
- as for time: $t \leq 10^{(0.17 + 0.85(Mm - 4.0))/1.3} - 0.3$
- as for magnitude: $Ma < Mm - 1.0$

where L, t, Mm and Ma represent an epicentral distance from the main shock, time in days from occurrence of a main shock, magnitude of a mainshock, and that of an aftershock, respectively. These relations were derived from Utsu's (1970) and consider the exponential decaying in number and magnitude of aftershocks.

4. Earthquake source zones

4.1. *Earthquake source zones geometry*

A seismic source zoning for the PILOTO Project region was produced joining the data from the complete and homogenized earthquake catalogue, the geological input (particularly from national active fault maps) and geodynamic models (fig. 4). Qualified judgment and discussion between regional experts during the Second Workshop on Hazard Assessment (Quito, June 1997) played an important role in sources definition.

In the North Andean region four different seismotectonic environments were identified: seismic subduction zones, crustal seismic zones, transcurrent-transformant zones and volcanic seismogenic zones.

Seismic subduction zones – The following geologic features were considered in the definition of the zones:

i) Tectonic features in the oceanic plate: Nazca Cordillera, Mendaña Fracture zone, Carnegie Cordillera.

ii) Active volcanism at Southern Peru, Northern Chile, Northern Ecuador and Colombia.

iii) Contouring of the subducting slab in the Wadati-Benioff zone in two regions: 1) change from normal subduction (gently dipping of the subducting slab) in Northern Chile and Southern Peru region to abnormal subduction (abrupt change in slab dip, from 20°-35° to almost subhorizontal) in Central Peru and Southern Ecuador with the slab dipping strongly to the SW;

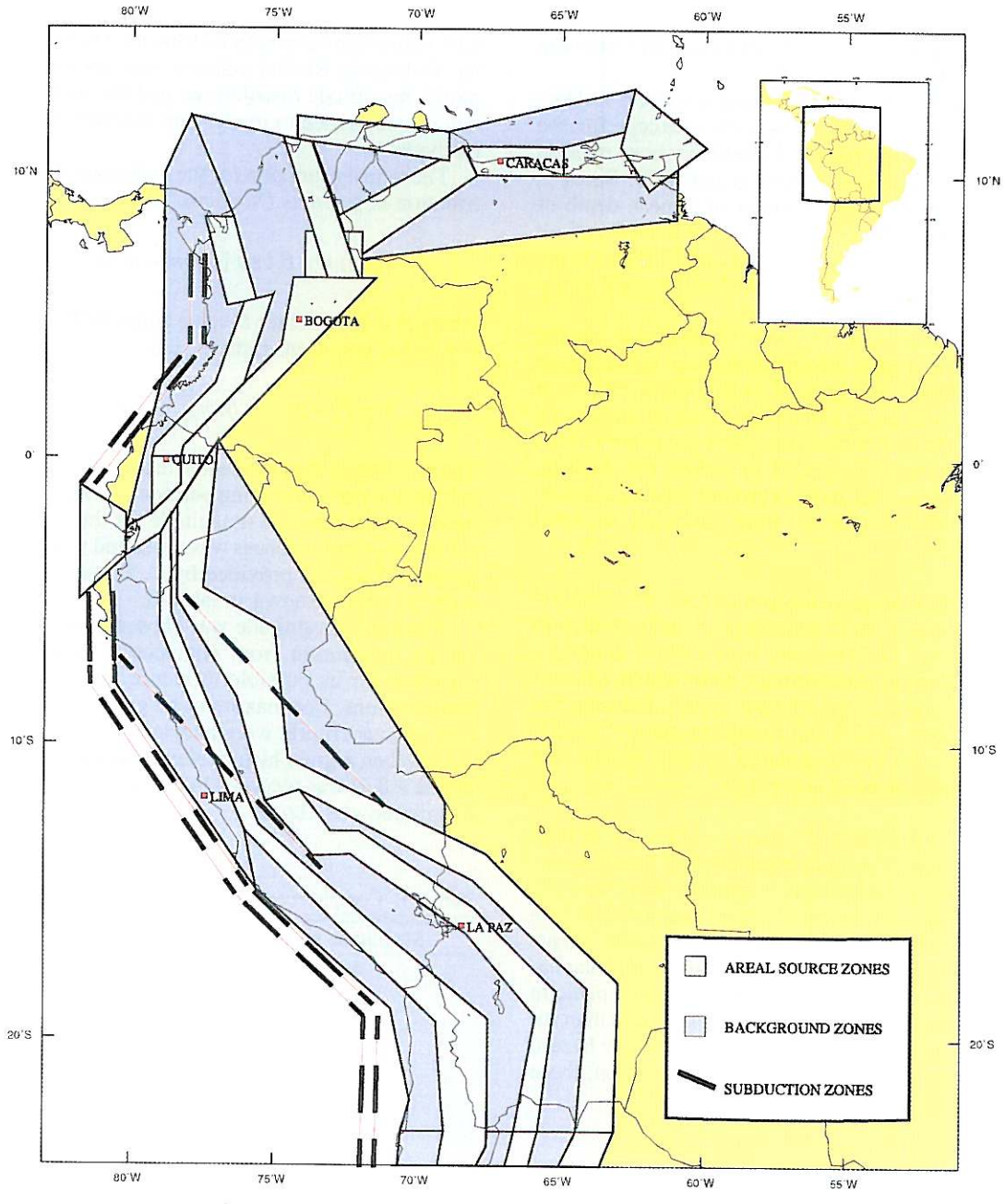

Fig. 4. North Andean region seismic sources

2) change from abnormal subduction in Southern Ecuador to normal subduction in Colombia with the slab dipping NE.

Geometry of the subduction sources follows the pattern of the trench axis, except for the Bucaramanga Nest in Colombia whose relation with subduction process is not clear. So, it is modeled as an areal source at a mean depth of 150 km. Subduction zones were treated as fault sources, except for Ecuador and El Pilar (Venezuela) zones which were modeled as areal zones.

Crustal seismic zones – To define crustal seismic zones information from active faults and seismicity maps of each country, results of microseismicity and paleoseismic studies, along with the tectonic and morphologic pattern of the region, was integrated to define the Andean, subandean and the background seismic sources. All crustal sources were modeled as areal sources.

Transcurrent-transformant zones – Detailed neotectonic and seismological field studies in the coast of Venezuela have clearly defined a transcurrent-transformant zone which concentrates most of the relative motion between the Caribbean and South American plates. The different sources associated to this system are modeled as areal sources.

Volcanic seismic zones – Although in both segments of normal subduction in South America active volcanism is present there has not been destructive earthquakes associated to volcanic phenomena, except for the many events accompanying the cone explosion of Huaynaputina volcano (Peru), which produced panic in the population for their frequency more than for their intensity. For this reason in seismic hazard assessment for the North Andean region, these type of sources are not considered.

4.2. *Seismic source characterization*

Seismic zones characterization was performed assuming an exponential model for magnitude distribution and a Poisson time occurrence model.

To characterize seismic activity of areal and fault sources the exponential truncated model of the Gutenberg-Richter relation was chosen to model magnitude distribution, and the average rate of occurrence to model time occurrence of earthquakes.

The density function for the exponential distribution is given as (McGuire, 1993)

$$f_M(m) = k\,\beta \exp\left[-\beta(m - m_0)\right]$$

where β is the Richter b-value times ln(10), m_0 is a lower bound magnitude, and

$$k = \left[1 - \exp\left[-\beta(m_{\max} - m_0)\right]\right]^{-1}.$$

The b-values of the exponential distribution were calculated after estimating periods of completeness for each range of magnitude for the whole catalogue. Completeness was evaluated with the program PILOTO provided by C. Bosse, GFZ, with the results shown in table II.

Minimum magnitude was chosen as 4.0 not for its importance from engineering point of view but for its possible influence in b-values computations. For maximum magnitude selection various criteria were adopted:

– When a great historical earthquake (magnitude ≥ 8.0) was recorded in the catalogue, this magnitude was chosen.

Table II. Completeness of the earthquake catalogue.

Magnitude range	Complete since
4.0	1960
4.5	1951
5.0	1940
5.5	1930
6.0	1922
6.5	1900
7.0	1886
7.5	1790
8.0	1700
8.5	1560
9.0	1470

– When no great earthquake was recorded, the maximum historical earthquake plus 0.5 units in magnitude was selected for the maximum magnitude earthquake.

– When doubts appeared concerning to historical magnitudes and some type of geologic or neotectonic indication or evidence was present, expert judgment was privileged.

For a more physical estimate of the maximum magnitude, the magnitude (M_W) to rupture length (L) equation of Dorbath *et al.* (1990) was used

$$M_W = 1.62 \log L + 4.44.$$

For maximum magnitudes, M_W was supposed similar to M_S.

Seismic characteristics for each source zone are shown in North Andean region seismic sources Annex.

5. Strong ground motion relations

Two attenuation equations for ground acceleration previously developed were used, one for crustal sources and another for subduction sources.

For crustal sources it was used the relation determined for Quijada *et al.* (1993):

$$\ln Acc = 5.40 + 0.36\, M_S - 0.86 \ln (R + 10)$$

$$\sigma (\ln Acc) = 0.66.$$

For subduction sources, it was used the relation derived by Saragoni *et al.* (1981):

$$\ln Acc = 7.74 + 0.71\, M_S - 1.6 \ln (R + 60)$$

$$\sigma (\ln Acc) = 0.5$$

where Acc is ground acceleration in cm/s^2.

6. Hazard computation method

A regional hazard map of the JUNAC region was produced, integrating information on seismicity, seismic source geometry and characterization and ground motion attenuation. To produce the hazard map the software FRISK88M (Risk Engineering, 1996) licensed *ad-hoc*, was used. It was decided to evaluate hazard for a 10% probability of exceedance in 50 years and the ground motion parameter chosen was acceleration.

FRISK88 calculates seismic hazard using the standard methodology described in McGuire (1993). The seismic hazard calculations are represented by the following equation, which is an application of the total probability theorem:

$$H(a) =$$

$$= \Sigma_i \nu_i \iint P[A > a/m, r]\, f_{Ri\backslash Mi}(r/m)\, f_{Mi}(m)\, dr\, dm$$

where the hazard $H(a)$ is the annual rate of earthquakes that produce a ground motion amplitude A higher than a. Here A represents peak ground acceleration. The summation extends over all source sets, ν_i is the annual rate of earthquakes (with magnitude higher than some threshold m_0) in source set i, and $f_{Mi}(m)$ and $f_{Ri\backslash Mi}(r/m)$ are the probability density functions on magnitude and distance. $P[A > a \,|\, m, r]$ is the probability that an earthquake of magnitude m at distance r produces a ground motion amplitude at the site which is greater than a.

Calculations of ground accelerations with a 10% probability of in 50 years were obtained at sites in a regular grid of 0.5 degrees. Various runs of the program were done to test the influence of different inputs like maximum magnitudes and geometries of some sources. Preliminary results were discussed with participants in PILOTO Project and modifications were done for the final version.

The final results are summarized in the map of fig. 5 with peak ground acceleration curves in m/s^2 each 0.1 units. The values for peak ground acceleration for the region run from about 6 m/s^2 at the Pacific coastal region of Peru to 0.5 m/s^2 at the eastern plains.

7. Discussion of hazard results

In general, the seismic hazard values obtained in the PILOTO Project are comparable to those of the probabilistic map of seismic hazard

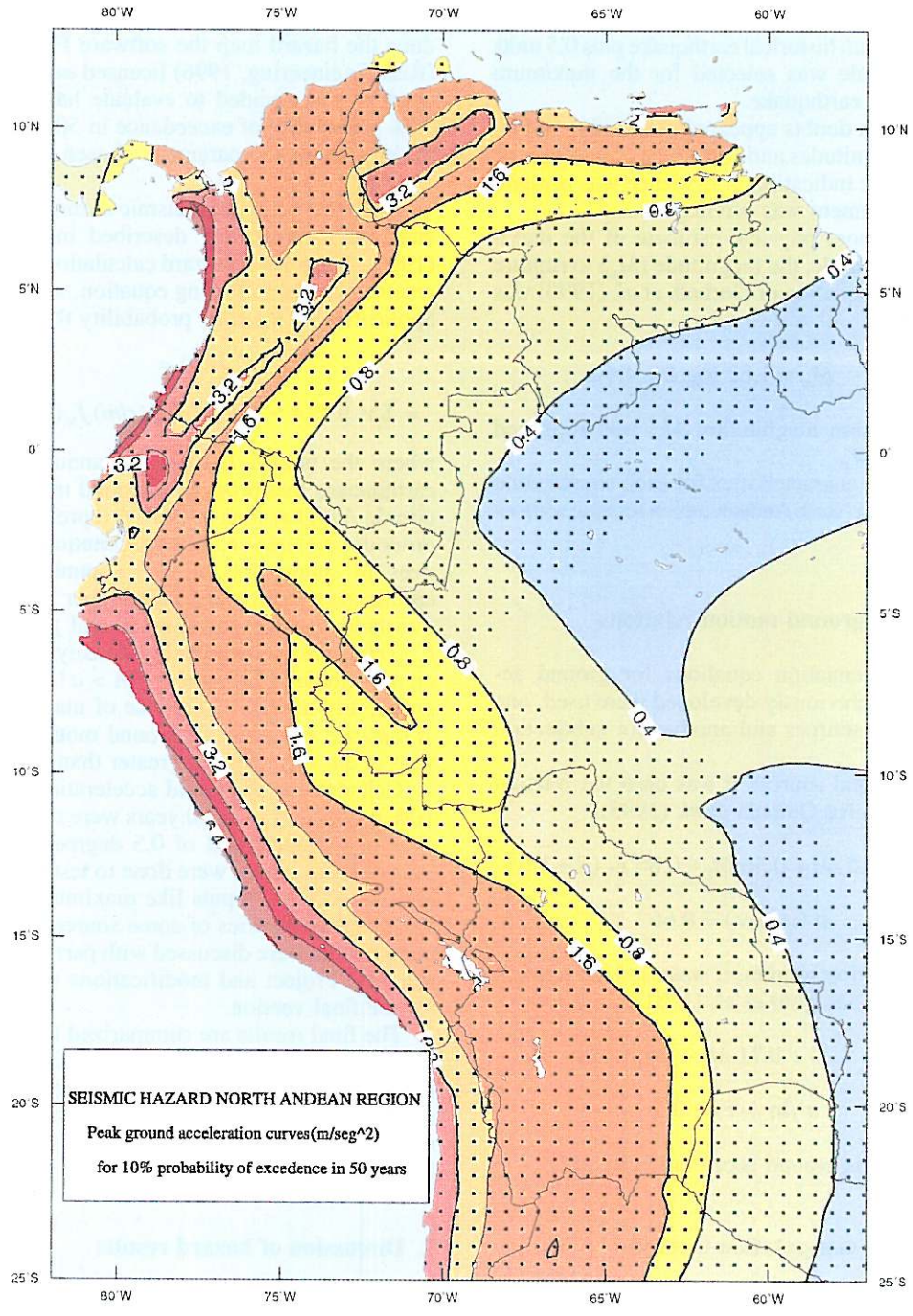

Fig. 5. Peak ground acceleration for the North Andean region (m/s^2).

for South America (CERESIS, 1996), except for the high values obtained in the coast of Peru and the low values at the coast of Chile. These differences are probably due to different choices of subduction zones geometry and assignation of the great historical subduction events to one or another section in the subduction zones. It should be emphasized the important amount of expert judgment involved in this type of estimations due to incomplete knowledge of seismic sources and processes.

As a final recommendation, something to do in the near future is to establish a logic tree including all uncertainties involved in seismic hazard assessment, to better judge the influence of a given parameter in ground motion estimation.

ANNEX. North Andean region seismic sources.

Geographical coordinates

Area sources coordinates

Code	Name	Coordinates
VE.1	Backgrd 1 Venezuela	69W 10.72N, 72.808W 8.57N, 73.8W 11.19N, 69.W 10.72N
VE.2	Backgrd 2 Venezuela	–69W 10.5N, –69.W 11.5N, –62.5W 13N, –62.7W 11.5N, –65W 11N, –68.5W 11N, –69W 10.5N
VE.3	Backgrd 3 Venezuela	–72.295W 7N, –68W 10N, –65W 10N, –62W 10N, –62W 9.5N, –61.4W 10N, –61W 10N, –61W 8.5N, –72.295W 7N
CO.1	Backgrd 1 Colombia	–77.5W 8.5N, –76.7W 5.4N, –76.1W 5.54N, –77.1W 2.65N, –79.2W 0.4N, –79.3W 0N, –78.3W 0N, –78.3W –1S, –79.3W –2S, –80.2W –2.5S, –78.91W 3N, –78.91W 10N, –78W 12N, –76.5W 8.5N, –77.5W 8.5N
CO.2	Backgrd 2 Colombia	–76.5W 8.5N, –75.7W 5.62N, –75.1W 5.8N, –76.1W 2.65N, –74.8W 4N, –74.4W 6.4N, –73.2W 6.4N, –74.8W 11.3N, –78W 12N, –76.5W 8.5N
CO.3	Nido Bucaramanga Colombia	–74W 8N, –72W 8N, –72W 6N, –74W 6N, –74W 8N
VE.4	Subduc Pilar Prof Venezuela	–63W 11N, –62.5W 13N, –60W 11N, –62W 9.5N, –63W 11N
CO.4	Cordillera Centrocc. Colombia	–79.2W 0.4N, –77.1W 2.65N, –76.1W 5.54N, –75.1W 5.8N, –76.1W 2.65N, –78.2W 0.4N, –78.3W 0N, –79.3W 0N, –79.2W 0.4N
CO.5	Murindo Colombia	–76.7W 5.4N, –77.5W 8.5N, –76.5W 8.5N, –75.7W 5.62N, –76.7W 5.4N
CO.6	B/manga-Stamarta Colombia	–73.2W 6.4N, –74.8W 11.3N, –73.8W 11.11N, –72.1W 6.4N, –73.2W 6.4N
VE.5	Bocono Venezuela	–72.8W 8.57N, –68.5W 11N, –68W 10N, .–72.29W 7N, –72.81W 8.52N
VE.6	Sansebastian Venezuela	–66.5W 11N, –65W 11N, –65W 10N, –68W 10N, –68.5W 11N
VE.7	Oca-Ancon Venezuela	–74.3W 12N, –69W 11.5N, –69W 10.5N, –74.3W 11.19N, –74.3W 12N
VE.8	El Pilar Venezuela	–65W 11N, –61W 12N, –61W 10N, –65W 10N, –65W 11N

Area sources coordinates (continued)

Code	Name	Coordinates
CO.7	Cordillera Oriental Colombia	–78.2W 0.4N, –74.8W 4N, –74.4W 6.4N, –71.5W 6.4N, –77.2W 0.3N, –78W –1S, –79W –2.7S, –80.2W –3.5S, –80.2W –2.5S, –79.3W –2S, –78.3W –1S, –78.3W 0N, –78.2W 0.4N
EC.1	Valle Interandino Ecuador	–79.3W 0N, –78.3W 0N, –78.3W –1S, –79.3W –2S
EC.2	Subduccion Ecuador	–81.8W –1S, –80.2W –2S, –80.2W –3.5S, –81.8W –5S
PE.1	Cordillera Occidental Peru Bolivia	–78.65W –2.05S, –78.6W –5.5S, –75.5W –12.8S, –67.46W –19.33S, –67.5W –23.5S, –69.0W –26.0S, –69.5W –26.0S, –69.1W –23.49S, –69W –23S, –69.3W –19.42S, –76W –13S, –79W –6S, –79W –2.7S, –78.65W –2.05S
PE.2	S. Peru N. Chile Bolivia	–76W –13S, –69.3W –19.42S, –69W –23S, –70.5W –23S, –70.2W –22.0S, –70.86W –19S, –75.6W –15S, –76W –13S
PE.3	Subandino Peru Bolivia	–77W 0.6N, –77.5W –4.6S, –75W –6S, –74.5W –10.5S, –67.54W –13.77S, –62.93W –18.11S, –63.07W –23S, –64.39W –23S, –64W –18.32S, –68W –14.68S, –74.1W –11.6S, –75.3W –12S, –76.3W –8.4S, –78.4W –5S, –78.4W –1.7S, –77W 0.6N
PE.4	Cord. Or. Sur Peru–Bolivia	–74.1W –11.6S, –73W –13S, –72W –13S, –68W –15.59S, –65.08W –18.41S, –65.71W –23S, –66.54W –23.0S, –65.81W –19.23S, –68.23W –16.48S, –72.3W –13.8S, –73.6W –13.85S, –75.3W –12S, –74.1W –11.6S
PE.5	Backgrd Costa Norte Peru	–79W –1.7S, –79W –6S, –76W –13S, –75.6W –15S, –80.5W –8S, –80.8W –3.85S, –79W –1.7S
PE.6	Backgrd Altiplano Peru Bolivia	–78.4W –1.7S, –78.4W –5S, –76.3W –8.4S, –75.3W –12S, –73.6W –13.85S, –72.3W –13.8S, –68.23W –16.48S, –65.81W –19.23S, –66.54W –23S, –67.46W –23S, –67.46W –19.33S, –75.5W –12.8S, –78.6W –5.5S, –78.65W –2.05S, –78.4W –1.7S
PE.7	Cord. Oriental Peru Bolivia	–74.1W –11.6S, –68W –14.68S, –64W –18.32S, –64.39W –23S, –65.71W –23.0S, –65.08W –18.41S, –68W –15.59S, –72W –13S, –73W –13S, –74.1W –11.6S
PE.8	Backgrd Oriente Peru Bolivia	–77W 0.6N, –69W –12S, –69W –13.5S, –74.5W –10.5S, –75W –6S, –77.5W –4.6S, –77W 0.6N
AR.1	Jujuy zone 2	–65.71W –23S, –66.2W –24.7S, –68.0W –26.0S, –68.8W –26.0S, –67.0W –24.7S, –66.54W –23.0S
AR.2	Jujuy zone 3	–63.07W –23S, –64.4W –26.0S, –66.0W –26.0S, –64.39W –23S
CH.1	Backgrd 1 Jujuy	–67.46W –23S, –66.54W –23S, –67.0W –24.7S, –68.8W –26.0S, –69.0W –26.0S, –67.50W –23.49S
AR.3	Backgrd 2 Jujuy	–64.39W –23S, –66.0W –26.0S, –68.00W –26.0S, –66.2W –24.7S, –65.71W –23.0S
CH.2	Backgrd 3 Jujuy	–69W –23S, –69W –26.0S, –70.8W –26S, –70.5W –23S
PE.9	Subduccion Superf. Centro 2 Peru	–73.3W –14.3S, –80.4W –7S

Fault sources coordinates

Code	Name	Coordinates
CH.3	Subduccion Superf. Chile	–72W –28S, –71.8W –19.25S
CH.4	Subduccion Prof. Chile	–71.5W –28.01S, –71.3W –19.26S
PE.10	Subduccion Superf. Sur Peru	–71.8W –19.25S, –76.3W –15.2S
PE.11	Subduccion Prof. Sur Peru	–71.47W –18.88S, –75.97W –14.83S
PE.12	Subduccion Superf. Centro 1 Peru	–76.3W –15.2S, –81.4W –8S
PE.13	Subduccion Prof. Centro 1 Peru	–75.89W –14.91S, –80.99W –7.71S
PE.14	Subduccion Prof. Centro 2 Peru	–71.1W –12.17S, –78.15W –4.872S
PE.15	Subduccion Superf. Norte Peru	–81.4W –8S, –81.5W –4.75S
PE.16	Subduccion Prof. Norte Peru	–80.55W –7.97S, –80.65W –4.72S
CO.8	Subduccion Prof. Colombia Ecuador	–81.3W –1S, –77.5W 4N
CO.9	Subduccion Superf. Colombia Ecuador	–81.8W –1S, –78.0W 4N
CO.10	Subduccion Superf. Colombia	–78.0W 4N, –78.00W 7.7N
CO.11	Subduccion Prof. Colombia	–77.5W 4N, –77.50W 7.7N

Seismicity parameters

Area sources seismicity parameters

Code	Name	Depth	Min. Mag.	Max. Mag.	NU	Beta
VE.1	Backgrd 1 Venezuela	15	4.0	6.5	0.43	2.06
VE.2	Backgrd 2 Venezuela	15	4.0	6.0	0.33	2.90
VE.3	Backgrd 3 Venezuela	15	4.0	7.0	1.29	1.69
CO.1	Backgrd 1 Colombia	15	4.0	7.4	1.11	1.22
CO.2	Backgrd 2 Colombia	15	4.0	7.0	1.29	1.69
CO.3	Nido Bucaramanga Colombia	150	4.0	6.5	10.68	3.24
VE.4	Subduc Pilar Prof. Venezuela	130	4.0	6.5	0.61	2.31
CO.4	Cordillera Centrocc. Colombia	15	4.0	7.5	0.49	0.97
CO.5	Murindo Colombia	15	4.0	7.5	1.12	1.66
CO.6	B/manga-Stamarta Colombia	15	4.0	6.0	0.43	1.93
VE.5	Bocono Venezuela	15	4.0	7.5	2.45	1.77
VE.6	Sansebastian Venezuela	15	4.0	8.5	0.30	1.27
VE.7	Oca-Ancon Venezuela	15	4.0	6.5	0.44	2.04
VE.8	El Pilar Venezuela	15	4.0	8.0	1.94	1.72
CO.7	Cordillera Oriental Colombia	15	4.0	8.5	3.03	1.54
VE.9	Pilar Subduccion Interm. Venezuela	60	4.0	7.0	0.73	1.52
EC.1	Valle Interandino Ecuador	15	4.0	7.5	1.25	1.68
EC.2	Subduccion Ecuador	35	4.0	8.0	3.59	1.64
PE.1	Cordillera Occidental Peru Bolivia	15	4.0	8.8	3.08	1.52

Area sources seismicity parameters (continued)

Code	Name	Depth	Min. Mag.	Max. Mag.	NU	Beta
PE.2	S. Peru N. Chile Bolivia	15	4.0	8.0	1.22	0.95
PE.3	Subandino Peru Bolivia	15	4.0	7.5	1.86	1.05
PE.4	Cord. Or. Sur Peru–Bolivia	15	4.0	8.0	0.98	1.20
PE.5	Backgrd Costa Norte Peru	15	4.0	8.0	1.42	1.31
PE.6	Backgrd Altiplano Peru Bolivia	15	4.0	8.0	0.46	1.05
PE.7	Cord. Oriental Peru Bolivia	15	4.0	7.5	0.39	1.33
PE.8	Backgrd Oriente Peru Bolivia	15	4.0	7.0	0.13	1.17
AR.1	Jujuy zone 2	15	4.0	6.5	0.03	0.46
AR.2	Jujuy zone 3	15	4.0	6.7	0.32	1.26
CH.1	Backgrd 1 Jujuy	15	4.0	7.5	0.05	1.17
AR.3	Backgrd 2 Jujuy	15	4.0	6.5	0.17	0.89
CH.2	Backgrd 3 Jujuy	15	4.0	7.3	0.62	1.37
PE.9	Subduccion Superf. Centro 2 Peru	115	4.0	8.0	0.18	1.55

Fault sources seismicity parameters

Code	Name	Dip	Min. Depth	Max. Depth	Min. Mag	Max. Mag	NU	Beta
CH.3	Subduccion Superf. Chile	20	2	20	4.0	8.8	0.89	1.36
CH.4	Subduccion Prof. Chile	35	21	250	4.0	8.8	13.29	1.71
PE.10	Subduccion Superf. Sur Peru	20	2	20	4.0	8.0	0.45	1.77
PE.11	Subduccion Prof. Sur Peru	35	21	250	4.0	8.8	23.78	1.97
PE.12	Subduccion Superf. Centro 1 Peru	12	2	20	4.0	8.0	0.51	1.32
PE.13	Subduccion Prof. Centro 1 Peru	30	21	120	4.0	8.8	13.29	1.71
PE.14	Subduccion Prof. Centro 2 Peru	22	116	155	4.0	8.0	2.90	1.43
PE.15	Subduccion Superf. Norte Peru	12	2	20	4.0	8.0	0.27	1.19
PE.16	Subduccion Prof. Norte Peru	25	21	210	4.0	8.8	5.09	1.82
CO.8	Subduccion Prof. Colombia Ecuador	30	30	180	4.0	7.8	7.06	1.86
CO.9	Subduccion Superf. Colombia Ecuador	30	2	30	4.0	8.7	1.71	1.35
CO.10	Subduccion Superf. Colombia	30	2	30	4.0	8.0	2.26	1.48
CO.11	Subduccion Prof. Colombia	30	30	180	4.0	8.0	2.62	1.71

REFERENCES

CERESIS, Centro Regional de Sismología para América del Sur (1985): *Catálogo de Terremotos para América del Sur*, edited by B. ASKEW and S.T. ALGERMISSEN, *CERESIS,* vol. 4, p. 269.

CERESIS, Centro Regional de Sismología para América del Sur (1996): 25 años: Convenio Multinacional, 30 años: Acuerdo Bilateral Perú-Unesco, p. 8.

CERESIS, Centro Regional de Sismología para América del Sur (1996): Actualización del Catálogo Sísmico Regional para América del Sur, magnetic copy.

DE METS, C., R.G. GORDON, D.F. ARGUS and S. STEIN (1990): Current plate motions, *Geophys. J. Int.*, **101**, 425-478.

DORBATH, L., A. CISTERNAS and C. DORBATH (1990): Quantitative assessment of great earthquakes in Peru, *Bull. Seismol. Soc. Am.*, **80**, 551-576.

FREYMUELLER, J., J. KELLOGG and V. VEGA (1993): Plate motions in the North Andean region, *J. Geophys. Res.*, **98** (B12), 21853-21863.

JORDAN, T.E., B.L. ISACKS, R.W. ALLMENDINGER, J.A. BREWER, V.A. RAMOS and C.L ANDO (1983): Andean tectonics related to geometry of subducted Nazca plate, *Geol. Soc. Am. Bull.*, **94**, 341-361.

GUTENBERg, B. and C.F. RICHTER (1956): Earthquake magnitude, intensity, energy and acceleration, *Bull. Seismol. Soc. Am.*, **46**, p. 131.

MAEDA, K. (1996): The use of foreshocks in probabilistic prediction along the Japan and Kuril Trenches, *Bull. Seismol. Soc. Am.*, **86** (1A), 242-254.

MCGUIRE, R. (1993): Computations of seismic hazard, *Ann. Geofis.*, **36** (3-4), 181-200.

NORABUENA, E.O., J.A. SNOKE and D.E. JAMES (1994): Structure of the subducted Nazca plate beneath Peru, *J. Geophys. Res.*, **99** (B5), 9215-9226.

PENNINGTON, W. (1981): Subduction of the EastermPanama basin and seismotectonics of Northwestern South America, *J. Geophys. Res.*, **86** (B11), 10753-10770.

PILOTO PROJECT (1997): EU-DG12 Ct. CII* 94-0103 Pilot Project for Regional Earthquake Monitoring and Seismic Hazard Assesment, *Final Report*, Editor Coordinator D. GIARDINI.

QUIJADA, P., E. GAJARDO, M. FRANKE, M. KOZUCH and J. GRASES (1993). Análisis de amenaza sísmica de Venezuela para el nuevo mapa de zonificación con fines de ingeniería, *Memorias del Octavo Seminario Latinoamericano de Ingeniería Sismo-Resistente, July 1993, Mérida.*

RISK ENGINEERING (1996): *FRISK88M Version 1.70 User's Manual.*

SARAGONI, R., CREMPIAN and M. ARAYA (1981): Características de los movimientos fuertes en Chile, *Publ. SES I-2/81* (164).

SUÁREZ, G., P. MOLNAR and B. BURCHFIEL (1983): Seismicity, fault plane solutions, depth of faulting, and active tectonics of Peru, Ecuador, and Southern Colombia, *J. Geophys. Res.*, **88** (B12), 10403-10428.

TANNER, J.G. and J.B. SHEPHERD (1997): Seismic hazard in Latin American and the Caribbean, Instituto Panamericano de Geografía e Historia, *Final Report*, vol. 1, 4.

UTSU, T. (1970): Aftershocks and earthquake statistics (2) – further investigation of aftershocks and other earthquake sequences based on a new classification of earthquake sequences, *J. Fac. Sci. Hokkaido Univ. Ser.*, **7** (3),197-266, in K. MAEDA (1996).